2016 IEEE Intelligent Vehicles Symposium (IV)
Gothenburg, Sweden, June 19-22, 2016

Probabilistic Rectangular-Shape Estimation for Extended Object Tracking

Peter Broßeit[1], Matthias Rapp[2], Nils Appenrodt[3] and Jürgen Dickmann[3]

***Abstract*— This paper presents new methods for the representation of a vehicle's contour by an oriented rectangle, also known as the bounding box. The parameters of this bounding box are originally modeled probabilistically by a single multivariate Gaussian distribution. This approach incorporates the sensor uncertainties, where the problem of estimating the parameters of this distribution from range measurements is addressed. Additionally, a transformation of the parameters into the measurement space is introduced. This representation is used to perform probabilistic updates by new measurements. The proposed method can handle strong parameter changes which might be affected by object occlusion. Experiments on real-world data demonstrate the robustness and accuracy of the probabilistic approach integrated in a tracking framework incorporating the Doppler measurements of automotive radars and laser measurements.**

I. Introduction

A reliable environmental perception of the ego-vehicle's surroundings involving dynamic objects such as other road users is essential for autonomously-driving vehicles. While there are various object types that have to be considered, other vehicles are of utmost importance in any traffic scenario.

These vehicles have a certain position and current motion state relative to the ego-vehicle and a spatial expansion. To provide safe maneuver planning, these parameters must be estimated for each object. This estimation is based on measurement data i.e. from laser sensors, which are affected by the sensor uncertainties. Additionally, object occlusions and a limited field of view makes this a challenging task. In the automotive domain, the assumption of *extended objects* is valid since vehicles have a spatial expansion, resulting in multiple measurements of a single object. The state-of-the-art tracking methods are Bayesian recursive filters, where the Random Finite Set approach applies the Bayesian tracking method to multiple objects. An overview of current approaches for extended objects is given in [1].

An essential component of any probabilistic extended object tracking framework is the extent or shape model. This component must represent the object's state and, equally important, related uncertainties with a sufficient accuracy to allow measurement association and updates. Otherwise, the entire tracking process will be unstable because of model errors. In the field of automotive extended object tracking, it is common to approximate the shape of a vehicle by an orientated rectangle known as *orientated bounding box*.

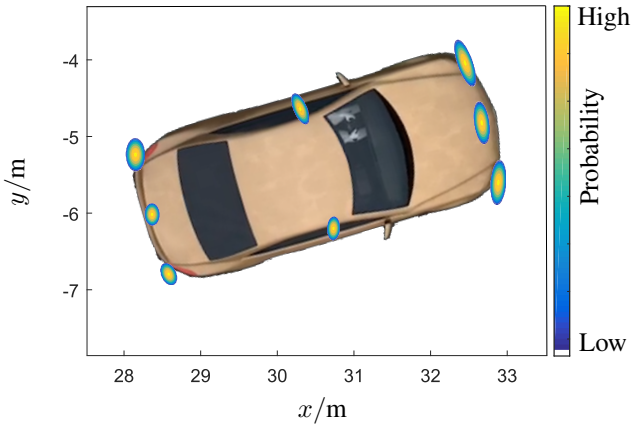

Fig. 1. For several points on the probabilistic rectangle's contour, the calculated covariances from the rectangle-distribution are visualized. These local distributions approximate not only the vehicle's shape but also all uncertainties and correlations.

At this stage, there is no approach known to the authors that estimates the full covariance matrix of the parameters for a vehicle's orientated bounding box of a vehicle. Focusing on the extend model, this paper contributes an estimation method for the orientated rectangle modeled as a multivariate normal distribution which provides the full covariance matrix. Furthermore, this method involves update routines for an orientated rectangle to process new measurements. One advantage of the covariance matrix estimation is the explicit probabilistic modeling of the *position-extent correlation* through the corresponding correlation coefficients. These coefficients allow to observe a dependency between the estimation of the vehicle's shape and the position, a fact that several authors have pointed out [2], [3]. This dependency is referred to as position-extent correlation in the following and appears in the update step if a change in object's size leads to a change in the position or vice versa. The structure of this paper is as follows: A review over existing shape models is given in Section II. In Section III the problem and prerequisites are described. Section IV derives the probabilistic bounding box model. This model is integrated in a tracking framework in Section V. The proposed method is evaluated on real-world sensor data in

[1]Peter Broßeit is with Department for Environment Perception, Daimler AG, Germany and Institute of Photogrammetry and Remote Sensing, TU Dresden, Germany peter.brosseit@daimler.com

[2] Matthias Rapp is with Institute of Measurement, Control and Microtechnology of Ulm University, Ulm, Germany matthias.rapp@uni-ulm.de

[3]Nils Appenrodt and Jürgen Dickmann are with the Department for Environment Perception, Daimler AG, Germany nils.appenrodt@daimler.com, juergen.dickmann@daimler.com

Section VI. The conclusion in Section VII summarizes the most important contributions of this paper.

II. Related Work

The problem of estimating the shape of an extended object has been addressed by several authors in the past. Petrovskaya et al. use a Rao-Blackwellized particle filter to estimate the object's position, orientation and rectangular-shape [2]. The authors introduce an additional vector to compensate changes in the position caused by the position-extent correlation. However, a full covariance matrix of the state is not estimated. Another approach based on an *Extended Kalman filter* is presented by Kmiotek and Ruichek [3]. This method estimates variances for each single state parameter but does not regard correlation between them. Instead of a covariance matrix, a single vector with variances is obtained. The position-extent correlation is not addressed by the tracking. A Gaussian Mixture approximation of the rectangle is used in the measurement model by Granström et al. [4]. Here, a set of 2D normal distributions is used to represent the contour, which may lead to a loss of correlation information. For the update step, each measurement has to be associated with exactly one normal distribution.

Other authors address the case of elliptical-shapes with *Random Matrices* (RM) [5]–[7] and *Random Hypersurface Models* (RHM) [8]. With RM the shape is modeled by the mean and covariance of a spatial distribution. They have been successfully integrated in different Bayesian frameworks. For example, a *Probability Hypothesis Density Filter* for multiple object tracking is described in [9]. The elliptic RHM is parametrized by the center, the *Cholesky decomposition* of a semi-positive definite matrix for the shape and the respective uncertainties by a normal distribution. Baum et al. compare RM and elliptical RHM [10]. Both models are well-suited for tracking approaches because they provide closed-form measurement updates and explicit modeling of state covariances. Concerning vehicle tracking, a drawback of these methods is the limitation to elliptical shapes, which is not the best approximation of vehicles.

To overcome this shape restriction, Baum et al. generalize RHMs to any star-convex shape [11]. This model is feasible for Bayesian inference and explicit representation of parameter uncertainty such as the elliptical representation. However, the performance of this method is still crucially dependent on the initialization. Another general approach is based on object-local occupancy grid maps [12]. Here, an object-centered grid map is tracked and the probability of occlusion for each cell is estimated recursively. Therefore, it is not restricted to a specific shape, but comes with high computational requirements. A method to model the shape using a group of sample points is introduced by Wyffels and Campbell [13]. This publication also provides a recent overview of state-of-the-art models.

III. Problem Formulation

To focus on the essential elements of the proposed method, a single observed object and already segmented measurements are considered in the following. But the extension to multiple objects is straight-forward and allows the integration in an appropriate multiple object Bayesian framework. The uncertainties of the measurements lead to uncertainties in the bounding box estimation. To consider these uncertainties, the bounding box is modeled as a multivariate normal distribution with state vector $\boldsymbol{\mu} \in \mathbb{R}^5$ and covariance matrix $\boldsymbol{\Sigma}^{\boldsymbol{\mu}} \in \mathbb{R}^{5\times5}$. In the following, $\boldsymbol{\Sigma}^{\boldsymbol{x}}$ denotes the covariance matrix with the corresponding mean $\boldsymbol{x}$. The parameter state of the bounding box

$$\boldsymbol{\mu} = [x_M, y_M, l, w, \alpha]^\intercal \tag{1}$$

consists of the position of the center (x_M, y_M), the half-length l, the half-width w, and the orientation α. A measurement point $\boldsymbol{m} = [x, y]^\intercal \in \mathbb{R}^2$ is given in 2-dimensional Cartesian coordinates. It is assumed that more than one measurement is received from the observed object due to the extended object assumption. The number of obtained measurement points associated with the object is denoted by n in the following. If range and bearing measurements are given, they have to be transformed to 2-dimensional Cartesian coordinates in advance. The set of measurements is concatenated in a single vector $\boldsymbol{L} \in \mathbb{R}^{2n}$. The corresponding covariance matrix is denoted by $\boldsymbol{\Sigma}^{\boldsymbol{L}} \in \mathbb{R}^{2n\times2n}$. Moreover, it is necessary to estimate the vehicles motion state $\boldsymbol{u} = [v, \omega]^\intercal \in \mathbb{R}^2$, which is parametrized by the velocity into the heading direction v and the change of orientation ω. The corresponding covariance matrix is termed $\boldsymbol{\Sigma}^{\boldsymbol{u}} \in \mathbb{R}^{2\times2}$.

IV. Probabilistic Bounding Box

This section addresses the problem of estimating the bounding box parameters $\boldsymbol{\mu}$ and corresponding covariance matrix $\boldsymbol{\Sigma}^{\boldsymbol{\mu}}$ using measurements of consecutive scans. For the estimation method, an appropriate measurement model is introduced in Subsection IV-A. The estimation is carried out by an adjustment computation method which minimizes the least square errors, presented in Subsection IV-B. The transformation described in Subsection IV-C utilizes the shape model for recursive updates. The motion model from Subsection IV-D allows the prediction of the state. Subsection IV-E explains the initialization of the parameters in more detail.

A. Measurement Model

To compute an optimal estimation for the parameters, a mapping between the $\boldsymbol{\mu}$-space and the $\boldsymbol{L}$-space is needed. The purpose of the measurement model is to predict the measurements for a $\boldsymbol{\mu}$-realization. Because the measurements are samples from the visible vehicle contour, an ideal measurement $\hat{\boldsymbol{m}}$ is predicted based on an actual measurement $\boldsymbol{m}$. This ideal measurement is assumed to be the closest point on the contour, which is the orthogonal projection on the bounding box. This ideal measurement is given by

$$\hat{\boldsymbol{m}}(\boldsymbol{\mu}, \boldsymbol{m}) = \begin{bmatrix}\hat{x}\\ \hat{y}\end{bmatrix} = \begin{bmatrix}d\cdot\cos\bar{\alpha} + x\\ d\cdot\sin\bar{\alpha} + y\end{bmatrix} \tag{2}$$

with

$$d = \rho - \cos\left(\bar{\alpha} - \arctan\left(\frac{y - y_M}{x - x_M}\right)\right) \cdot \sqrt{(x - x_M)^2 + (y - y_M)^2}\,.$$

The Euclidean distance $\|\hat{\boldsymbol{m}}(\boldsymbol{\mu}, \boldsymbol{m}) - \boldsymbol{m}\|$ between the predicted $\hat{\boldsymbol{m}}(\boldsymbol{\mu}, \boldsymbol{m})$ and the actual measurement $\boldsymbol{m}$ is exactly d. The parameters ρ and $\bar{\alpha}$ are dependent on the side association. For the front and rear, ρ is l or w for the two other sides. The bounding box sides are denoted by a counter clockwise incrementing line identification $i \in \{0 \dots 3\}$ where 0 is the front. Using this line id, the term $\bar{\alpha}$ is equal to $\alpha + \frac{\pi}{2} \cdot i$.

The probability of an arbitrary measurement point conditioned on a bounding box distribution $p(\boldsymbol{m}, \boldsymbol{\Sigma^m} | \boldsymbol{\mu}, \boldsymbol{\Sigma^\mu})$ is defined by the Euclidean distance d and the corresponding variance. For this distance, the uncertainty is modelled by a normal distribution. The according variance is derived by the laws of error propagation [14] as

$$\sigma_d^2 = \boldsymbol{J^e} \cdot \begin{bmatrix} \boldsymbol{J^d \Sigma^\mu J^{d\intercal}} & \boldsymbol{0} \\ \boldsymbol{0} & \boldsymbol{\Sigma^m} \end{bmatrix} \cdot \boldsymbol{J^{e\intercal}}\,, \tag{3}$$

where $\boldsymbol{J^d} \in \mathbb{R}^{2\times 5}$ is the Jacobian matrix of (2) with respect to $\boldsymbol{\mu}$. The Jacobian matrix $\boldsymbol{J^e} \in \mathbb{R}^{1\times 4}$ is the deviation of the Euclidean distance with respect to $\hat{\boldsymbol{m}}$ and $\boldsymbol{m}$. The probability is defined as:

$$p(\boldsymbol{m}, \boldsymbol{\Sigma^m} | \boldsymbol{\mu}, \boldsymbol{\Sigma^\mu}) = \frac{1}{\sigma_d \sqrt{2\pi}} \cdot \mathrm{e}^{-\frac{1}{2}\left(\frac{d}{\sigma_d}\right)^2} \tag{4}$$

It is common to assume that the measurements are independent, so the overall likelihood of all measurements $\boldsymbol{L}$ is

$$p(\boldsymbol{L}, \boldsymbol{\Sigma^L} | \boldsymbol{\mu}, \boldsymbol{\Sigma^\mu}) = \prod_{i=1}^{n} p(\boldsymbol{m_i}, \boldsymbol{\Sigma^{m_i}} | \boldsymbol{\mu}, \boldsymbol{\Sigma^\mu})\,. \tag{5}$$

This likelihood is maximized to achieve the best parameters of the bounding box for measurements $\boldsymbol{L}$. This is done by a geometrical adjustment based on least squares in the next subsection. Figure 2 visualizes the likelihood for a realization of a probabilistic bounding box.

B. Adjustment Computation

The computation of the best parameters $\boldsymbol{\mu}_{\text{opt}}$ is achieved through a general least square method [14] which minimizes the residuals ν of x and y according to (2). As the measurements are concatenated in $\boldsymbol{L}$, these residuals are collected in $\boldsymbol{v}$:

$$\boldsymbol{v} = [\dots, \nu_i^x, \nu_i^y, \dots]^\intercal$$

Therefore, the following equation system is set up:

$$\underbrace{\begin{bmatrix} d_1 \cdot \cos\bar{\alpha}_1 + x_1 \\ d_1 \cdot \sin\bar{\alpha}_1 + y_1 \\ \vdots \\ d_j \cdot \cos\bar{\alpha}_j + x_j \\ d_j \cdot \sin\bar{\alpha}_j + y_j \end{bmatrix} - \begin{bmatrix} (x_1 + \nu_1^x) \\ (y_1 + \nu_1^y) \\ \vdots \\ (x_j + \nu_j^x) \\ (y_j + \nu_j^y) \end{bmatrix} = 0}_{\mathcal{M}} \tag{6}$$

For the optimization, the norm of the vector $\boldsymbol{v}$ is minimized

$$\boldsymbol{v}_{\text{opt}} = \underset{\boldsymbol{v}}{\operatorname{argmin}} \|\boldsymbol{v}\|$$

with respect to the equation system $\mathcal{M}$.

The general least square adjustment computation requires an approximate solution $\hat{\boldsymbol{\mu}}$, where in this context the predicted state can be used. For initialization and line association of the measurement points see Subsection IV-E. Furthermore, the two Jacobian matrices $\boldsymbol{J^\mu} = \frac{d\boldsymbol{M}}{d\boldsymbol{\mu}} \in \mathbb{R}^{2n\times 5}$ and $\boldsymbol{J^\nu} = \frac{d\boldsymbol{M}}{d\boldsymbol{\nu}} \in \mathbb{R}^{2n\times 2n}$, which are derived with respect to the state or residuals, respectively, are required. Additionally, $\hat{\boldsymbol{L}}$ is the vector of the predicted measurements as given by (2) and $\boldsymbol{L}$ the vector of the pure measurements. The difference is $\boldsymbol{l} = \boldsymbol{L} - \hat{\boldsymbol{L}}$. Using these parameters, the estimate can be computed as follows:

$$\begin{bmatrix} \boldsymbol{k} \\ \Delta\boldsymbol{\mu} \end{bmatrix} = \begin{bmatrix} \boldsymbol{J^\nu \Sigma^L J^{\nu\intercal}} & \boldsymbol{J^\mu} \\ \boldsymbol{J^{\mu\intercal}} & \boldsymbol{0} \end{bmatrix}^{-1} \begin{bmatrix} \boldsymbol{l} \\ \boldsymbol{0} \end{bmatrix} \tag{7}$$

$$\boldsymbol{\mu} = \hat{\boldsymbol{\mu}} + \Delta\boldsymbol{\mu} \tag{8}$$

The corresponding covariance matrix $\boldsymbol{\Sigma^\mu}$ is calculated from the measurement covariance matrix $\boldsymbol{\Sigma^L}$ considering the functional dependencies. The cofactor matrix $\boldsymbol{Q^\mu}$, which is $\boldsymbol{\Sigma^\mu}$ scaled by a scalar factor, is computed as:

$$\boldsymbol{Q^\mu} = \left(\boldsymbol{J^{\mu\intercal}}\left(\boldsymbol{J^\nu \Sigma^L J^{\nu\intercal}}\right)^{-1}\boldsymbol{J^\mu}\right)^{-1} \quad \in \mathbb{R}^{5\times 5} \tag{9}$$

To obtain $\boldsymbol{\Sigma^\mu}$, the reference variance s^2 has to be calculated from the residuals $\boldsymbol{v}$:

$$\boldsymbol{v} = \boldsymbol{\Sigma^L J^{\nu\intercal} k} \quad \in \mathbb{R}^{2n} \tag{10}$$

$$s^2 = \frac{\boldsymbol{v^\intercal \Sigma^L}^{-1}\boldsymbol{v}}{2 \cdot n - 5} \tag{11}$$

The covariance matrix $\boldsymbol{\Sigma^\mu}$ is given by:

$$\boldsymbol{\Sigma^\mu} = s^2 \cdot \boldsymbol{Q^\mu}\,. \tag{12}$$

This covariance matrix then concludes the variances as well as the corresponding correlation coefficients of the estimated parameters $\boldsymbol{\mu}$.

C. Bounding Points

The estimated parameters $\boldsymbol{\mu}_{\text{opt}}$ can be integrated in a Bayesian filter framework in a straight-forward way. However, the problem of this approach is that it cannot handle rapid changes in $\boldsymbol{\mu}$. These changes occur, when the bounding box is only partly observed, caused by occlusions or the limited field of view. In such cases the bounding box parameters, which are extracted in consecutive measurements, would not follow the assumed distributions. This prevents the application of direct Bayesian filtering . To address this problem, an alternative update routine is proposed. The bounding box distribution is transformed into an equivalent distribution of discrete points on the bounding box's edge. This set of

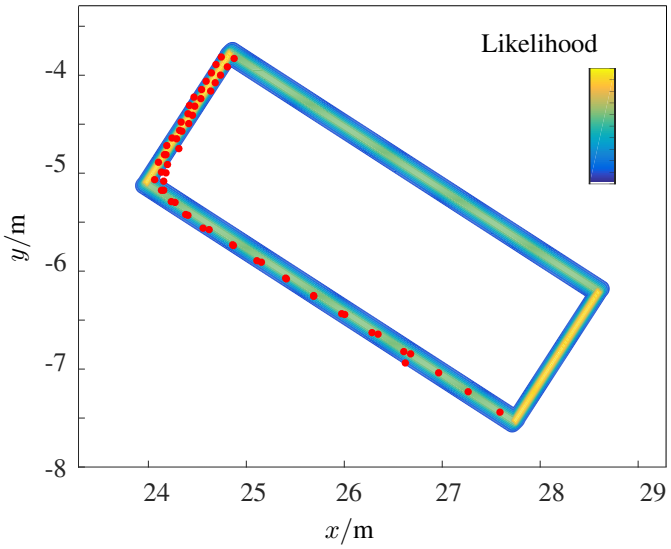

Fig. 2. The Likelihood of measurements for a probabilistic bounding box, considering uncertainties and correlations. This parameters are calculated via adjustment calculation using the measurements and bounding points depicted in Figure 3. The measurements are visualized by red dots.

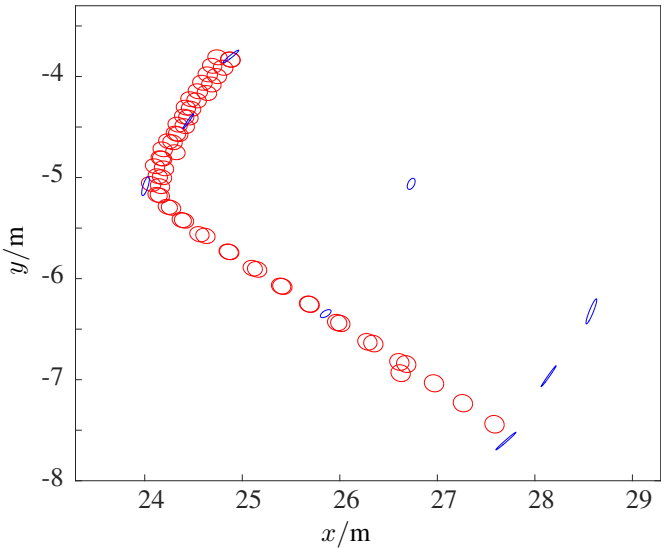

Fig. 3. The error ellipses of the measurement points $\boldsymbol{L}$ (red) and the bounding points $\boldsymbol{P}$ (blue).

synthetic points $\boldsymbol{P}$ contains the corner points as well as the side medians for a parameter set $\boldsymbol{\mu} = [x_M, y_M, l, w, \alpha]^\intercal$:

$$\boldsymbol{P} = \begin{bmatrix} l & l & l & 0 & -l & -l & -l & 0 \\ -w & 0 & w & w & w & 0 & -w & -w \end{bmatrix}^\intercal \cdot \begin{bmatrix} \cos(\alpha) & -\sin(\alpha) \\ \sin(\alpha) & \cos(\alpha) \end{bmatrix} + \begin{bmatrix} x_M & 0 & x_M & 0 & x_M & 0 & x_M & 0 \\ 0 & y_M & 0 & y_M & 0 & y_M & 0 & y_M \end{bmatrix}^\intercal \tag{13}$$

The corresponding covariance matrix is calculated via the general law of propagation of variances [14] using the Jacobian matrix of $\boldsymbol{P}$:

$$\boldsymbol{\Sigma}^{\boldsymbol{P}} = \boldsymbol{J}^{\boldsymbol{P}} \cdot \boldsymbol{\Sigma}^{\boldsymbol{\mu}} \cdot \boldsymbol{J}^{\boldsymbol{P}\intercal} \tag{14}$$

Through (13), the rectangle distribution can be transformed to the measurement space. The transformation (14) of the variances and correlations allows a sufficient approximation of the probabilistic characteristics. The parameter update is achieved by the adjustment computation introduced in Subsection IV-B using the measurements and the bounding points as input parameters. This allows the selective cancellation of specific bounding points as a preprocessing before the adjustment computation. The cancellation is necessary if there are strong contradictions between the prior shape estimation and the measurements which are not accounted for by the distributions. As outlined before, this may occur because of occlusions. The bounding points approximation is shown in Fig. 3 together with a set of measurements.

D. Motion Model

A motion model is used for the state prediction from the last measurements at time $t-1$ to the consecutive at time t. For vehicle tracking, it is common to use the *constant-turn model with polar velocity* [15]. The model requires the position of the vehicle's rotation center, which is the center of the rear axis (x_R, y_R). This is approximated by shifting x_M and y_M along the length axis by $1/4$ of the length of the estimated bounding box. Experiments show that this approximation is legitimate for most automobiles. Therefore, this point has to be shifted back to the rectangular center after the prediction. To also predict the full bounding box covariance by error propagation, the model is extended by the width w and the length l of the bounding box:

$$\begin{aligned} \boldsymbol{\mu_t} &= g(\boldsymbol{\mu_{t-1}}, \boldsymbol{u_t}) \\ &= \begin{bmatrix} x_{R_{t-1}} + \frac{2}{\omega_t} v_t \sin\left(\frac{\omega_t \Delta_t}{2}\right) \cos\left(\alpha_{t-1} + \frac{\omega \Delta_t}{2}\right) \\ y_{R_{t-1}} + \frac{2}{\omega_t} v_t \sin\left(\frac{\omega_t \Delta_t}{2}\right) \sin\left(\alpha_{t-1} + \frac{\omega \Delta_t}{2}\right) \\ l_{t-1} \\ w_{t-1} \\ \alpha_{t-1} + \omega_t \Delta_t \end{bmatrix} \end{aligned} \tag{15}$$

where Δ_t is the elapsed time between two measurements and the indices $t-1$ and t names the temporal validity of the estimated parameters. Thus, the covariance matrix prediction is given by

$$\boldsymbol{\Sigma}_{\boldsymbol{t}}^{\boldsymbol{\mu}} = \begin{bmatrix} \boldsymbol{J}_{\boldsymbol{\mu_t}}^{\boldsymbol{g}} & \boldsymbol{J}_{\boldsymbol{u_t}}^{\boldsymbol{g}} \end{bmatrix} \begin{bmatrix} \boldsymbol{\Sigma}_{\boldsymbol{t-1}}^{\boldsymbol{\mu}} & \boldsymbol{0} \\ \boldsymbol{0} & \boldsymbol{\Sigma}_{\boldsymbol{t}}^{\boldsymbol{u}} \end{bmatrix} \begin{bmatrix} \boldsymbol{J}_{\boldsymbol{\mu_t}}^{\boldsymbol{g}\intercal} \\ \boldsymbol{J}_{\boldsymbol{u_t}}^{\boldsymbol{g}\intercal} \end{bmatrix}, \tag{16}$$

where the Jacobian matrices of (15) with respect to $\boldsymbol{\mu}$ and $\boldsymbol{u}$ are used. Additionally, the process noise of the motion parameters has to be incorporated by the corresponding covariance $\boldsymbol{\Sigma}_{\boldsymbol{t}}^{\boldsymbol{u}}$ [15].

E. Initialization and Line Association

To set up the equation system (6), the association of each measurement to a side of the rectangular must be determined. For this purpose line-feature extraction is performed with the split-and-merge algorithm, which is fast and robust as

demonstrated in [16]. Next, a regression is performed for each line and the variances of the line parameters are compared with a threshold. For high variances the underlying measurement set is not likely to represent the line segments sufficiently but rather contains a critical amount of clutter. Therefore, the respective set of measurements is removed. The remaining points are associated to the closest side if a prediction of $\boldsymbol{\mu}$ is available. If the object is observed the first time, the association is determined by a state-of-the-art bounding box fit. In this paper, the line-based method described by Kmiotek and Ruichek is used [3], but any other rectangular-fit can be utilized (for example [17]). The retrieved solution $\hat{\boldsymbol{\mu}}$ is subsequently used for the association and serves as approximate solution in the adjustment calculation (Subsection IV-B).

F. Efficient Computation

The computation of $\boldsymbol{\mu}$ and $\boldsymbol{\Sigma}^{\boldsymbol{\mu}}$ can be done very efficiently by exploiting the sparse structure of $\boldsymbol{\Sigma}^{\boldsymbol{L}}$ and $\boldsymbol{J}^{\boldsymbol{\nu}}$. So, the equation (7) can be solved by a LU-decomposition, which avoids matrix inversion and is very fast for sparse matrices. It can be shown that the matrix $\boldsymbol{Q}^{\boldsymbol{\mu}}$ is the lower-right 5×5 block matrix of the inverse in (7). The values of $\boldsymbol{Q}^{\boldsymbol{\mu}}$ are calculated using the adjugate and the equation $\boldsymbol{A}^{-1} = \mathbf{adj}(\boldsymbol{A}) / \det(A)$ [14]. To take advantage of $\boldsymbol{Q}^{\boldsymbol{\mu}}$'s symmetry, only one triangle of the adjugate actually has to be calculated. Therefore only $15+1$ determinants are needed to set up $\boldsymbol{Q}^{\boldsymbol{\mu}}$ - avoiding any inversion.

V. Single Vehicle Tracking

The proposed probabilistic rectangular model is integrated in a single object tracking framework to estimate $\boldsymbol{\mu}$ and $\boldsymbol{u}$ from consecutive measurements. As intelligent vehicles are the main application, a sensor setup that includes radar and laser sensors is assumed. To use the full potential of this sensor configuration, $\boldsymbol{u}$ is estimated based on the radar data $\boldsymbol{R}$ which involves a measurement of the radial velocity known as *Doppler velocity*. There are sophisticated methods based on the measured Doppler profile of an extended object [18]. The shape parameters $\boldsymbol{\mu}$ are estimated based on laser measurements, because of the higher spatial accuracy.
This tracking framework uses a Rao-Blackwellized particle filter, very similar to the one described in [2]. The factorization of the belief is

$$p(\boldsymbol{\mu_t}, \boldsymbol{u_t} | \boldsymbol{L_t}, \boldsymbol{R_t}) = p(\boldsymbol{u_t} | \boldsymbol{L_t}, \boldsymbol{R_t}) p(\boldsymbol{\mu_t} | \boldsymbol{u_t}, \boldsymbol{L_t}) \,, \qquad (17)$$

where $p(\boldsymbol{\mu_t} | \boldsymbol{u_t}, \boldsymbol{L_t})$ is calculated using the probabilistic bounding box model scheme with each particle:

1) Sample $\boldsymbol{u_t} \sim \mathcal{N}(\hat{\boldsymbol{u}}_{\boldsymbol{t}}, \boldsymbol{\Sigma}^{\boldsymbol{u}}_{\boldsymbol{t}})$
2) Prediction of $\boldsymbol{\mu_t}$ and $\boldsymbol{\Sigma}^{\boldsymbol{\mu}}_{\boldsymbol{t}}$ from $\boldsymbol{\mu_{t-1}}$, $\boldsymbol{\Sigma}^{\boldsymbol{\mu}}_{\boldsymbol{t-1}}$, $\boldsymbol{u_t}$ and $\boldsymbol{\Sigma}^{\boldsymbol{u}}_{\boldsymbol{t}}$ applying (15) and (16)
3) Transformation to bounding points distribution set $\boldsymbol{P}$ and $\boldsymbol{\Sigma}^{\boldsymbol{P}}$ using (13) and (14)
4) Cancellation of inconsistent bounding points
5) Update by adjustment calculation proposed in Subsection IV-B using $\boldsymbol{P}$, $\boldsymbol{\Sigma}^{\boldsymbol{P}}$, $\boldsymbol{L_t}$ and $\boldsymbol{\Sigma}^{\boldsymbol{L}}_{\boldsymbol{t}}$
6) Calculate particle weight according to (5)

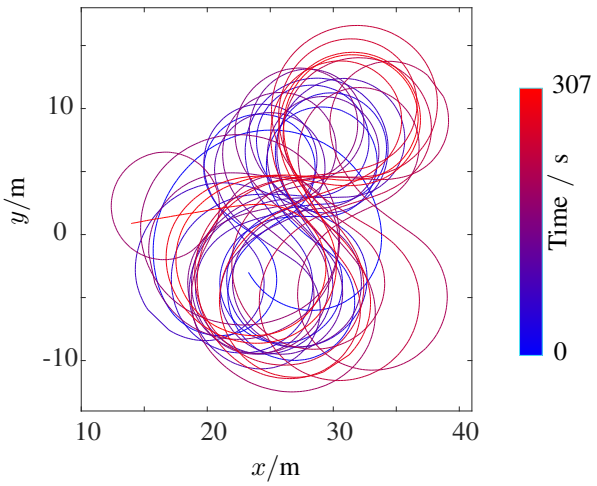

Fig. 4. The path of the observed vehicle in the examined scene.

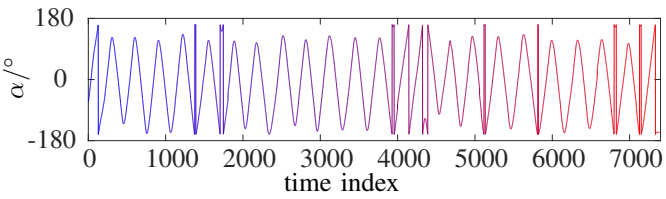

Fig. 5. The orientation of the observed vehicle over time. The values are normalized to the interval $[-\pi; \pi]$.

In addition, adaptive resampling is performed, conditioned on the *effective sample size* [19]. Thus the set of particles approximates $p(\boldsymbol{u_t} | \boldsymbol{L_t}, \boldsymbol{R_t})$ and provides an estimate for $\boldsymbol{\mu_t}$. However, to use the potential of the Doppler measurements, an asynchronous radar-based update is incorporated. This is based on a recent approach [20] that allows the estimation of the motion parameters, constrained on prior information given by the vehicle's position and orientation estimates. The radar measurements are processed as follows:

1) Prediction of $\boldsymbol{\mu_t}$ and $\boldsymbol{\Sigma}^{\boldsymbol{\mu}}_{\boldsymbol{t}}$ from $\boldsymbol{\mu_{t-1}}$, $\boldsymbol{\Sigma}^{\boldsymbol{\mu}}_{\boldsymbol{t-1}}$, $\boldsymbol{u_{t-1}}$ and $\boldsymbol{\Sigma}^{\boldsymbol{u}}_{\boldsymbol{t-1}}$ applying (15) and (16)
2) With this prior, estimate $\boldsymbol{u_t}$ and $\boldsymbol{\Sigma}^{\boldsymbol{u}}_{\boldsymbol{t}}$ as described in [20]
3) Filter the estimates with an additional Kalman filter to increase robustness and accuracy

Hence, the motion parameters are tracked using the valuable Doppler information and not only by the geometry-based likelihood. As a consequence of the smaller search space, fewer particles are required.

VI. Experimental Results

The performance of the proposed method was evaluated using a laser scanner and two automotive radar sensors. The radar data is captured with 15 Hz while the laser has an update rate of 25 Hz. In the examined scenario, a single vehicle was observed by the sensors of a second vehicle for approximately five minutes. This resulted in a large dataset

TABLE I

ERRORS OF THE ESTIMATED BOUNDING BOX PARAMETERS

Parameter		$\in \boldsymbol{\mu}$	RMSE	STD	MAX	MEAN
Position	/m	x	0.08	0.07	0.27	0.05
		y	0.10	0.10	0.52	-0.01
Orientation	/°	α	1.73	1.17	10.95	1.28
Length	/m	l	0.16	0.05	0.44	-0.15
Width	/m	w	0.14	0.08	0.34	-0.12

containing about four million laser measurements and about 240 000 radar detections. The laser sensor measures data in four different layers or under different vertical angles. In a preprocessing step, the measurements of these layers are merged into a synthetic 2D-scan. Both vehicles, the sensor platform as well as the observed vehicle, are equipped with high-precision navigation units. This system consists of an *Inertial Measurement Unit* for accurate motion measurement that is combined with a *Differential Global Navigation Satellite System*. The system serves as ground truth in the experiment. The path traversed by the observed vehicle is depicted in Fig. 4, while the ego-vehicle is positioned at the coordinate origin. Figure 5 shows the course of the orientation over time, illustrating that this is a highly dynamic scene, which challenges the tracking.

In the experiment, the parameters $\boldsymbol{\mu}$ of the bounding box of the observed vehicle are estimated using the data obtained from the sensors. These parameters are estimated using the tracking framework as described in the previous Section V. For the particle filter, the total number of particles was set to 100 for the experiments.

The resulting root-mean-squared errors and the standard deviations are summarized in Table I. Moreover, the mean and the maximum of the errors are displayed. Table I shows that the position of the observed vehicle can be estimated with a very small mean error of 0.05 m for the x-position and -0.01 m for y-position. The standard deviations for both estimations are below 0.1 m. In this experiment, the worst estimation for the position parameters is below 0.5 m. The orientation of the bounding box was estimated as well. The mean error for this parameter is only 1.28 °, where the standard deviation has a value of 1.2 °. The scattering of the errors of the position and orientation is also visualized by boxplots in Fig. 6. The parameters provided by the manufacturer were used as ground truth for the length and width. The standard deviation attained for the length is 0.05 m and for the width it is 0.08 m. A priori, a bias of the size parameters is expected, because the estimated rectangle is not covering the full extent. Instead, it is the best fitting rectangle with respect to the real shape of the observed object. This effect can be seen by the bias of -0.15 m for the length and -0.12 m for the width. Figure 7 illustrates the evolution of the length and width parameters over time. This figure shows that the estimation is stable and that there are no remarkable outliers present.

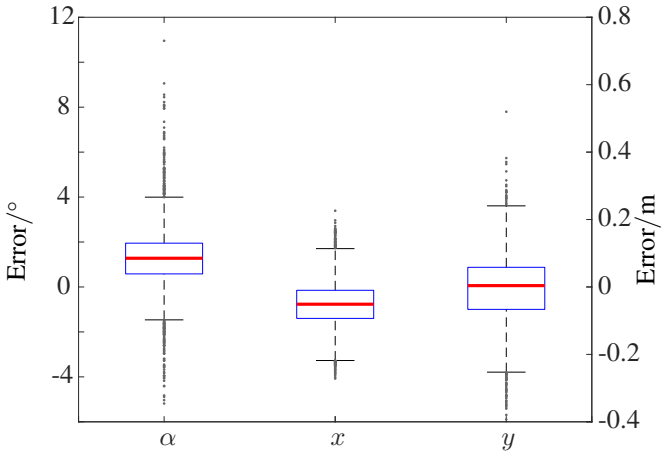

Fig. 6. Boxplots of the orientation and position errors.

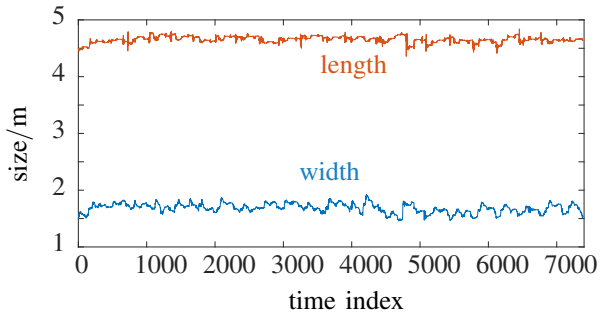

Fig. 7. The estimated length and width of the vehicle.

VII. CONCLUSION

This paper presents a new probabilistic shape model for rectangular extended object tracking. For this probabilistic bounding box, a measurement model is derived which allows determining the likelihood of measurements involving state and measurement uncertainties. A state estimation method is proposed based on adjustment calculation, which considers the probabilistic nature of measurements. The calculation is done efficiently by exploiting the sparse structure of the matrices involved. The method leads to a full covariance matrix for the bounding box parameters. This covariance matrix completely reflects the impact of measurement uncertainties on the parameter uncertainties and correlations. Moreover, this shape model is integrated in a tracking framework using radar and laser data. This tracking utilizes Doppler measurements to estimate the motion parameters of the observed vehicle. The proposed method is evaluated based on a large real-world data set. The experiments show that a very good accuracy is obtained for all bounding box parameters. For the position parameters, the RMSE is less than 0.1 m and for the orientation less than 1.7 °. The length and width could be estimated with high accuracy. The results show that this method is feasible for the perception of dynamic objects in the field of intelligent vehicles.

REFERENCES

[1] L. Mihaylova, A. Y. Carmi, F. Septier, A. Gning, S. K. Pang, and S. Godsill. Overview of Bayesian sequential Monte Carlo methods for group and extended object tracking. *Digital Signal Processing*, 25:1–16, 2014.

[2] A. Petrovskaya and S. Thrun. Model based vehicle detection and tracking for autonomous urban driving. *Autonomous Robots*, 26(2-3):123–139, 2009.

[3] P. Kmiotek and Y. Ruichek. Representing and Tracking of Dynamics Objects using Oriented Bounding Box and Extended Kalman Filter. *IEEE Conference on Intelligent Transportation Systems, Proceedings, ITSC*, pages 322–328, 2008.

[4] K. Granström, S. Reuter, D. Meissner, and A. Scheel. A multiple model PHD approach to tracking of cars under an assumed rectangular shape. *International Conference on Information Fusion*, 2014.

[5] W. Koch. Bayesian approach to extended object and cluster tracking using random matrices. *IEEE Transactions on Aerospace and Electronic Systems*, 44(3):1042–1059, 2008.

[6] M. Feldmann and D. Franken. Advances on Tracking of Extended Objects and Group Target Using Random Matrices. *International Conference on Information Fusion*, (1):1029–1036, 2009.

[7] M. Feldmann and W. Koch. Comments on "Bayesian approach to extended object and cluster tracking using random matrices". *IEEE Transactions on Aerospace and Electronic Systems*, 48(3):1687–1693, 2012.

[8] M. Baum and U. D. Hanebeck. Extended Object and Group Tracking with Elliptic Random Hypersurface Models. In *Conference on Information Fusion*, pages 1–8, 2010.

[9] K. Granstrom and U. Orguner. A phd filter for tracking multiple extended targets using random matrices. *IEEE Transactions on Signal Processing*, 60(11):5657–5671, 2012.

[10] M. Baum, M. Feldmann, D. Fränken, U. D. Hanebeck, and W. Koch. Extended Object and Group Tracking: A Comparison of Random Matrices and Random Hypersurface Models. In *Proceedings of the IEEE ISIF Workshop on Sensor Data Fusion: Trends, Solutions, Applications*, 2010.

[11] M. Baum and W. D. Hanebeck. Shape Tracking of Extended Objects and Group Targets with Star-Convex RHMs. In *International Conference on Information Fusion*, 2011.

[12] M. Schutz, N. Appenrodt, J. Dickmann, and K. Dietmayer. Multiple extended objects tracking with object-local occupancy grid maps. In *International Conference on Information Fusion*, pages 1–7, 2014.

[13] K. Wyffels and M. Campbell. Joint tracking and non-parametric shape estimation of arbitrary extended objects. *International Conference on Robotics and Automation*, pages 3360–3367, 2015.

[14] C. D. Ghilani. *Adjustment Computation - Spatial Data Analysis*. John Wiley & Sons, Hoboken, New Jersey, 2010.

[15] X. Rong, Li and V. P. Jilkov. Survey of Maneuvering Target Tracking. Part I. Dynamic Models. *IEEE Transactions on Aerospace and Electronic Systems*, 39(4):1333–1364, 2003.

[16] V. Nguyen, A. Martinelli, N. Tomatis, and R. Siegwart. A comparison of line extraction algorithms using 2D laser rangefinder for indoor mobile robotics. *International Conference on Intelligent Robots and Systems, IROS*, pages 1768–1773, 2005.

[17] F. Roos, D. Kellner, and K. Dietmayer. Estimation of the Orientation of Vehicles in High-Resolution Radar Images. In *International Conference on Microwaves for Intelligent Mobility (ICMIM), IEEE*, 2015.

[18] D. Kellner, M. Barjenbruch, J. Klappstein, and K. Dietmayer. Tracking of Extended Objects with High Resolution Doppler Radar. *IEEE Transactions on Intelligent Transportation Systems*, PP(99):1–13, 2015.

[19] M. S. Arulampalam, S. Maskell, N. Gordon, and T. Clapp. A tutorial on particle filters for online nonlinear/non-Gaussian Bayesian tracking. *IEEE Transactions on Signal Processing*, 50(2):174–188, 2002.

[20] P. Broßeit, D. Kellner, C. Brenk, and J. Dickmann. Fusion of Doppler Radar and Geometric Attributes for Motion Estimation of Extended Objects. In *Sensor Data Fusion: Trends, Solutions, Applications*, 2015.